BIOCHEMISTRY
including biophysical chemistry & molecular biology

Article

pubs.acs.org/biochemistry

Osmolyte Effects on the Self-Association of Concanavalin A: Testing Theoretical Models

Thomas R. Silvers and Jeffrey K. Myers*

Department of Chemistry, Davidson College, Box 7120, Davidson, North Carolina 28035, United States

Supporting Information

ABSTRACT: The formation and stability of protein−protein interfaces are of obvious biological importance. While a large body of literature exists describing the effect of osmolytes on protein folding, very few studies address the effect of osmolytes on protein association and binding. The plant lectin concanavalin A (ConA), which undergoes a reversible tetramer-to-dimer equilibrium as a function of pH, was used as a model system to investigate the influence of nine osmolytes on protein self-association. The stabilizing or destabilizing impacts of the osmolytes were evaluated from pH titrations combined with circular dichroism spectroscopy. Relative to the dimer, trimethylamine *N*-oxide, betaine, proline, sarcosine, sorbitol, sucrose, and trehalose all stabilized the ConA tetramer to varying extents. Glycerol had a negligible effect, and urea destabilized the tetramer. From multiple titrations in different osmolyte concentrations, an *m*-value (a thermodynamic parameter describing the change in the association free energy per molar of osmolyte) was determined for each osmolyte. Experimental *m*-values were compared with those calculated using two theoretical models. The Tanford transfer model, with transfer free energies determined by Bolen and co-workers, failed to accurately predict the *m*-values in most cases. A model developed by Record and co-workers, currently applicable only to urea, betaine, and proline, more accurately predicted our experimental *m*-values, but significant discrepancies remained. Further theoretical work is needed to develop a thermodynamic model to predict the effect of osmolytes on protein−protein interfaces, and further experimental work is needed to determine if there is a general stabilization by osmolytes of such interfaces.

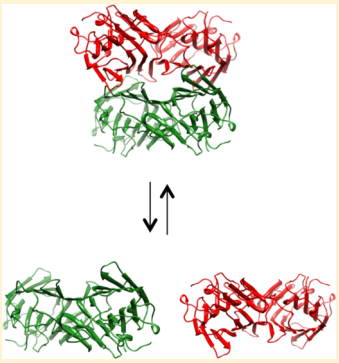

Biological function is intimately connected to macromolecular conformation. The stability of functional (biologically active) protein is strongly dependent on the environment of the protein. A key goal of protein science is the understanding of protein−solvent interactions and elucidating the thermodynamic effect of solvent additives on protein conformation. Osmolytes—small organic molecules that are accumulated inside the cells of many organisms—protect against a variety of osmotic stresses such as high salt concentrations, dehydration, or freezing.[1,2] Most osmolytes are considered to be *compatible*, meaning they do not interfere with the function of other molecules in the cell, and the evolution of such systems in a wide variety of organisms has been of particular interest. Osmolytes affect the thermodynamics of protein conformations, and a number of investigations have examined protein folding in osmolyte solutions.[3−10] Osmolytes generally stabilize folded protein structures, although to varying degrees. From work of Timasheff and others,[3,4,6,11] it is known that osmolytes (urea being a notable exception) generally promote preferential hydration of the protein. Thus, conformations that minimize protein−solvent interactions (i.e., folded states) are thermodynamically favored in the presence of osmolytes. Urea, on the other hand, destabilizes folded states, probably through direct interaction with the peptide backbone. The precise molecular mechanism of osmolyte action remains under investigation.[11−14]

While a large body of literature that describes the effect of osmolytes on the folding of proteins has accumulated, the effect of osmolytes on the stability of specific protein−protein interfaces (excluding aggregation) has gone relatively unexplored.[15,16] Given that similar types of noncovalent interactions and physical forces are thought to stabilize both folded proteins and protein−protein interfaces, we expect osmolytes to alter the thermodynamics of association as they do folding. We choose to use concanavalin A (ConA) as a convenient model to study the effect of osmolytes on the stability of protein−protein interfaces, since the protein undergoes a reversible dimer-to-tetramer equilibrium near neutral pH, and the association appears to involve minimal conformational changes in the subunits.

ConA is a legume lectin isolated from the jack bean (*Canavalia ensiformis*) and is one of the best-characterized lectins, as well as the first to be made commercially available.[17,18] ConA has a binding specificity for α-D-glucose and α-D-mannose sugars, with weak binding to monosaccharides and stronger binding to oligosaccharides such as those found on cell surface glycoproteins and glycolipids.[19] These biological properties have led to the utilization of ConA in a remarkable variety of biotechnological applications. ConA is a metalloprotein, requiring the presence of metal ions for proper binding function; each subunit of ConA contains one

Received: August 2, 2013
Revised: November 1, 2013
Published: November 11, 2013

   dx.doi.org/10.1021/bi401049s | *Biochemistry* 2013, 52, 9367−9374

manganese (Mn^{2+}) and one calcium (Ca^{2+}) ion. The tertiary structure of lectin monomers is devoid of α helices, consisting only of three antiparallel β-pleated sheets that form what is called the jelly roll fold (or jelly roll β-barrel domain), featuring a "back" six-stranded sheet, a "front" seven-stranded sheet, and a five-stranded "top" sheet.[20−23]

ConA exists as a tetramer near neutral pH, and this form predominates under most physiological conditions. Like most lectin tetramers, ConA can be described as a dimer of dimers that are formed by the overlap of the two back sheets upon each other.[21] ConA features a pattern of dimerization common to many lectins that is typified by a large dimeric interface (with extensive intersubunit interactions), the area of which is estimated to be 1150 Å^2 per monomer. Unfolding of the tetramer at pH 7 and the dimer at pH 5 with chemical denaturants has been studied.[24,25] The native tetramer is formed by two identical dimer−dimer interfaces that each bury nearly 2000 Å^2 of solvent-accessible surface area (SASA). The placement of the dimer−dimer interfaces near the edges of the slightly curved back sheets generates a large, water-filled cavity in the tetrameric state (Figure 1A). Dissociation of the tetramer to dimers can be driven by a change in pH from ∼7.5 to ∼5 in a reversible manner in which the subunit structure appears largely unperturbed. ConA binds saccharides with equal affinity in the tetrameric or dimeric forms,[26] and the tryptophan side chains appear to exist in the same environment in both forms;[27] thus, the subunits appear to be structurally unchanged upon tetramer formation. These results imply that the association free energy is dominated by formation of the dimer−dimer interfaces alone, instead of being coupled to conformational changes in the subunits. The pH dependence of the quaternary structure seems to be caused by the protonation of a single histidine side chain, with a pK_a of around 6.5;[28] His 51 and His 121 have been identified as likely candidates. The tetramer/dimer equilibrium has previously been studied using sedimentation equilibrium, light scattering, and spectroscopic methods.[26,28−31,26,28,30] Here, we use near-UV circular dichroism (CD), combined with pH titrations, to probe the quaternary structure to determine the free energy change of association the protein has in the presence of a variety of osmolytes.

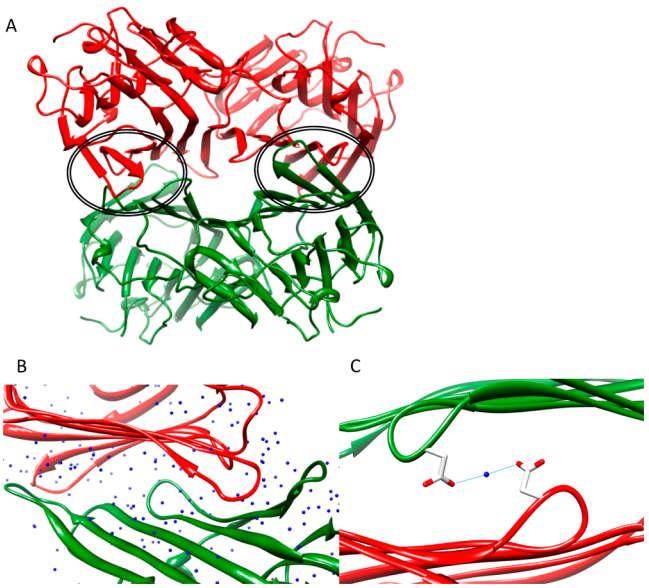

Figure 1. Representations of the ConA tetramer, produced with Chimera[64] from the pdb file 1jbc. (A) Overall ribbon diagram of the tetramer. Dimer−dimer interfaces are circled; the central water-filled cavity is evident between the interfaces. (B) Expanded view of one of the dimer−dimer interfaces, showing extensive hydration by water molecules (blue spheres) in the interfacial region. (C) Detailed view of one of the interfaces, showing a water molecule (water 581, blue sphere) "bridging", via hydrogen bonding (light blue lines), the side chains of Asp58 from two different subunits.

One method to predict and understand the thermodynamics of conformational changes in osmolyte solutions (or solvent additives in general) is the Tanford transfer model (TTM). The TTM has been refined in recent years by Bolen and co-workers to explain the effects of osmolytes on protein folding,[10] having originally been formulated by Tanford and co-workers.[32] In the TTM, a thermodynamic cycle is used to establish a relationship between the free energy changes for the conformational change and the free energies of transfer between solvents. A cycle for ConA association may be written as follows:

$$\begin{array}{ccc} & \Delta G^{w}_{2D\rightarrow T} & \\ 2\ D_w & \rightleftharpoons & T_w \\ \Delta G_{tr,2D}\ \Big\updownarrow & & \Big\updownarrow\ \Delta G_{tr,T} \\ 2\ D_{os} & \rightleftharpoons & T_{os} \\ & \Delta G^{os}_{2D\rightarrow T} & \end{array}$$

where T represents tetramer, D represents dimer, the w subscript denotes species in aqueous buffer, os denotes species in osmolyte solution, and tr denotes transfer free energies. Thus, to predict the change in $\Delta G_{T\rightarrow 2D}$ caused by adding osmolyte, we can utilize the transfer free energies for dimer and tetramer from water to osmolyte solution (the two side arms of the cycle): $\Delta\Delta G_{2D\rightarrow T} = \Delta G_{tr,T} - \Delta G_{tr,2D}$. If the osmolyte concentrations are 1 M, we get a thermodynamic quantity known as the *m*-value.

The *m*-value describes the dependence of ΔG on osmolyte, on a per molar basis, and was originally proposed by Pace to describe the denaturation of folded proteins by urea or other denaturants.[33,34] The simple linear relationship between free energy and denaturant or osmolyte concentration generally holds for both denaturants[34−36] and osmolytes.[8,37] Here we define the *m*-value thusly:

$$\Delta G_{2D\rightarrow T} = \Delta G^{\circ}_{2D\rightarrow T} - m[\text{osmolyte}] \quad (1)$$

such that a positive *m* represents stabilization of the tetramer relative to the dimer (we refer to $\Delta G_{2D\rightarrow T}$ as the association free energy). The transfer model relies on several assumptions, mainly involving treatment of solubility data to determine the transfer free energies, thermodynamic group additivity, and modeling the denatured state. Despite these assumptions the model has been remarkably successful at predicted *m*-values for a wide variety of osmolytes for a number of diverse proteins. As reported by Bolen et al.,[10] prediction of *m*-values for 51 monomeric ligand-free proteins resulted in excellent correspondence with experimentally determined *m*-values. Another successful method for predicting *m*-values has been developed by Record and co-workers.[13,38,39] Their model uses data from vapor pressure osmometry or solubility studies to generate interaction parameters between osmolytes and a library of

dx.doi.org/10.1021/bi401049s | *Biochemistry* 2013, 52, 9367−9374

model compounds. These data are then parsed into contributions from different functional groups, normalized by the surface area presented to the osmolyte. This model is more detailed than the transfer model, in that one can determine whether the osmolyte in question is preferentially included or excluded from particular groups in the biomolecule of interest. In this work, we address the applicability of the transfer model and Record's model to protein association, and the general ability of osmolytes to stabilize protein−protein interfaces.

METHODS

Preparation of ConA Solutions. ConA, prepared from *Canavalia ensiformis* (jack bean) and lyophilized, was purchased from Sigma. The commercial preparation was found to contain a significant fraction of hydrolyzed subunits; thus, additional purification was required. The method for the preparation of fully intact ConA has been described previously.[40,28] A 10 mg/mL solution of ConA was prepared in 5 mM sodium acetate (pH = 2.3). The solution was dialyzed against 1% ammonium bicarbonate (pH = 7.9) for 10−12 h at 37 °C, after which the solution was centrifuged for 20 min at 25000*g* to remove precipitates. The supernatant was passed through a 0.22 μm filter and extensively dialyzed against ConA storage buffer (50 mM sodium phosphate, 0.50 M NaCl, 0.2 mM $CaCl_2$, 0.2 mM $MnCl_2$, 0.1 mM NaN_3, pH = 6.5). Solutions prepared in this manner were stable for weeks at 4 °C. Concentrations of stock solutions were determined with UV absorbance spectroscopy, using an extinction coefficient $E_{cm}^{1\%} = 11.4$.[18]

Spectroscopic Determination of the Free Energy Change of Association. Near-UV CD spectra of ConA at 20 °C in pH 7.5 buffer (50 mM potassium phosphate, 0.5 M NaCl) and pH 5.0 buffer (50 mM sodium acetate, 0.5 M NaCl) were collected using a Jasco J-815 spectropolarimeter using a 1.0 cm path length quartz cuvette with a bandwidth of 1.5 nm. The temperature was held constant by a Peltier-type temperature controller (Quantum Northwest). Buffer blanks were subtracted in each case.

For titrations, samples of ConA were prepared at 0.5 mg/mL in titration buffer (50 mM acetate/50 mM phosphate, 0.5 M NaCl, pH 7.5) with or without osmolytes. Urea and trimethyamine *N*-oxide (TMAO) concentrations were determined using refractometry,[4,41] and all other osmolyte solutions were prepared gravimetrically. TMAO solutions were purified according to the method presented by Scholtz and Celinski.[42] ConA samples were subjected to pH titration starting at pH ≈ 7.5 and ending near pH ≈ 5.0 using a 6.05 M HCl solution as a titrant; samples were held at 20 °C and stirred. At each pH, the CD signal was determined at a wavelength of 284.0 nm over a measuring time of 60 s after 10 min of equilibration, using a bandwidth of 5.0 nm. The data were averaged to determine the mean CD signal at each particular pH; these values were then corrected to take into account the small dilution of the sample from the addition of the HCl solution. To determine the precise pH of the sample after addition of acid, mock titrations were carried out with the exact concentrations of buffer and osmolyte present in the CD samples, using a pH meter and mimicking the equivalent additions of acid.

For each titration, the resulting CD signal versus pH curve was used to fit the following equation:

$$Y = Y_T + \frac{\Delta Y}{1 + 10^{[n(\mathrm{pH}-\mathrm{pH}_{mid})]}} \quad (2)$$

where Y is the observed signal, Y_T is the signal of the tetramer, ΔY is the change in signal from tetramer to dimer, pH_{mid} is the observed pH midpoint (which can be thought of as an apparent pK_a), and n is the number of protons dissociating per dimer (both Y_T and ΔY contain a slope and an intercept, to account for small linear variations of signal as a function of pH that may be present independent of tetramer formation). In all the fits, the value for n was always close to 2; therefore, we fixed $n = 2$ for the final fits to reduce the number of floating parameters. The pH midpoint of the curve (where the fraction of chains in dimeric form was equal to 0.5) was then used as described below to determine the association free energy change.

According to Senear and Teller, ConA association can be described with the following simple linked equilibria:[28]

$$2D(2H^+) \rightleftarrows 2D + 4H^+ \rightleftarrows T + 4H^+$$

where $D(2H^+)$ represents protonated dimer, D represents deprotonated dimer, and T represents tetramer. This system gives the following relationship (derivable using Wyman's theory of linked functions[43]) between the relevant equilibrium constants and pH:

$$\ln K_{app} = \ln K_{assoc} - 4\ln(1 + 10^{-\mathrm{pH}}/10^{-\mathrm{p}K_a}) \quad (3)$$

where K_{app} is the apparent association constant, K_{assoc} is the association constant for deprotonated dimers, and the pK_a of the relevant side chain is taken to be 6.55, as determined by Senear and Teller.[28] The following relationship is present between the fraction dimer f_D and the apparent K:

$$K_{app} = (1 - f_D)/(2f_D^{\,2}C) \quad (4)$$

where C represents the concentration of dimer units. Utilization of eqs 3 and 4 with the experimental value of pH_{mid} (the pH at which $f_D = 0.5$) allows the determination of the association constant for deprotonated dimers to form tetramer and therefore also the association free energy. Multiple separate titrations of ConA in the absence of osmolytes were carried out to obtain an estimate of the error in the value of $\Delta G_{2D\rightarrow T}$ (±0.8 kJ/mol).

Calculation of *m*-Values Using the Transfer Model. The program NACCESS 2.1.1 (S. J. Hubbard and J. M. Thornton) was utilized to calculate the SASA of tetrameric and dimeric ConA, using the pdb file 3cna with a probe radius of 1.4 Å. Differences in SASA between the tetramer and two dimers were broken down into main chain surface and surfaces of the 20 different side chains. These were used to determine the number of peptide groups and side chains (of each type) buried in the dimer−dimer interfaces. Free energy of transfer values (from water to 1 M osmolyte solutions) for side chains and the main chain were used as given by Bolen and co-workers[44−46] to determine the total transfer free energy difference for tetramer and two dimers, equivalent to an *m*-value. These calculations may be carried out using an algorithm available on the web (http://sbl.utmb.edu/mvalue.html).

Calculation of *m*-Values Using the Model of Record and Co-Workers. Changes in SASA were calculated as above; *m*-values for urea, betaine, and proline were determined as described.[13,38,39]

RESULTS

A previous spectroscopic study of ConA association found only small changes in the far-UV CD spectrum of ConA at pH 5 and 7, but a significant change in the Cotton effect of the aromatic

dx.doi.org/10.1021/bi401049s | *Biochemistry* 2013, 52, 9367−9374

residues was noted near 280 nm.[29] Because this study likely used ConA that was partially hydrolyzed, we repeated CD measurements and also recorded fluorescence emission spectra of protein purified via precipitation of hydrolyzed subunits (see Methods). We noted only small changes in the fluorescence and far-UV CD spectra at pH 5 (dimer) and 7.5 (tetramer; data not shown), but a more noticeable change in the near-UV CD spectrum was observed (Figure 2). The major change appears

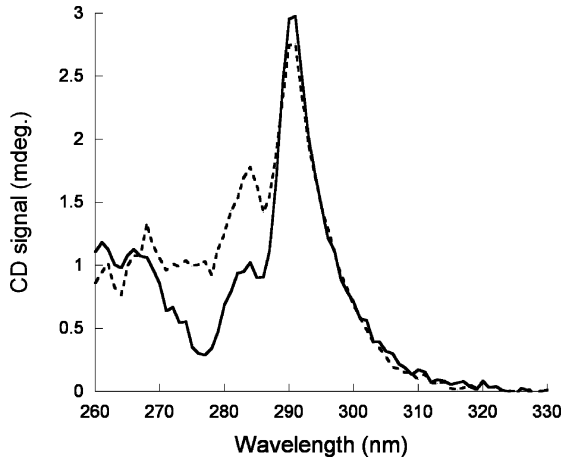

Figure 2. Near-UV CD spectra of ConA at pH 7.5 (tetramer, solid line) and 5.0 (dimer, dotted line). Protein concentration was 0.5 mg/mL, and the buffer was either 50 mM potassium phosphate at pH 7.5 or 50 mM sodium acetate at pH 5.0.

to be associated with a peak at 284 nm, likely due to environmental changes for several tyrosine side chains that are near the dimer−dimer interfaces. We have taken advantage of this spectroscopic signature to develop a simple assay for measuring the equilibrium constant for ConA association, namely, monitoring the CD signal at 284 nm as a function of pH.

Titrations starting at pH ≈ 7.5 and moving toward low pH produce a sigmoidal transition (Figure 3A). According to Senear and Teller, the tetramer-to-dimer transition is thought to be caused by the protonation of a single histidine on each subunit (probably histidine 51 or 121) whose pK_a is 6.55. We fit to these data a two-state model (see Methods) to determine the midpoint pH (pH_{mid}), at which half of the subunits are present in dimeric form. The midpoint pH can be thought of as an apparent pK_a distinct from the actual pK_a of the histidine, because protonation is linked to tetramer dissociation. For the association of two deprotonated dimers to form tetramer at 20 °C, we find an equilibrium constant of 1.7×10^7 for purified ConA, resulting in an estimate of the association free energy of −40.5 ± 0.8 kJ/mol. This compares well with the free energy change found by Senear and Teller (−37.8 kJ/mol) using sedimentation equilibrium with commercial protein purified in the same manner.[28] Thus, we are confident that we are monitoring the same dimer-to-tetramer equilibrium as Senear and Teller with our spectroscopic technique.

Titrations were repeated under identical conditions in the presence of a variety of osmolytes. In each case, we observed a sigmoidal dissociation curve as the pH was lowered. However, these curves were often shifted higher or lower in pH, indicating an alteration of the free energy of association caused by the osmolytes (Figure 3B). The free energy of association was determined in each case and plotted as a function of

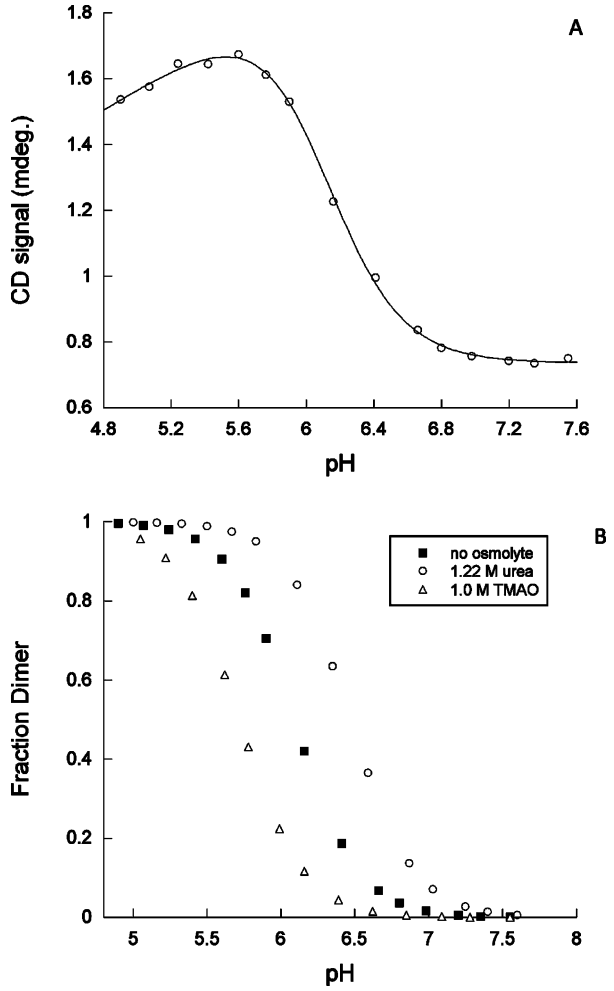

Figure 3. (A) pH titration of ConA followed by CD at 284 nm. Line results from fitting eq 1 with $n = 2$, giving a midpoint pH of 6.20. (B) Variation of the midpoint pH induced by osmolytes (urea at 1.22 M and TMAO at 1.00 M concentrations).

osmolyte concentration, as shown in Figure 4. In general, linear dependences of the free energy change on osmolyte concentration were observed, as expected. Linear functions were fit to these data to provide slopes representing *m*-values for each osmolyte, as given in Table 1. We also provide errors in the fitted *m*-values based on an average error in the association free energy of ±0.8 kJ/mol.

Experimentally, urea had a significant destabilizing effect on the tetramer, whereas TMAO significantly stabilized the tetramer, consistent with what has been observed for the folding of monomeric proteins. Of the other osmolytes, the carbohydrates (sorbitol, sucrose, and trehalose) had strong stabilizing effects, as did the methylamines betaine and sarcosine. Proline had a weaker stabilizing effect, and for glycerol the *m*-value was within error of zero.

The TTM was used to predict *m*-values for ConA association for each osmolyte, on the basis of the crystal structure of ConA (pdb code 3cna), as described in the Methods section. These values are compared to experimentally measured *m*-values in Table 1. Qualitatively, the model predicts the stabilizing or destabilizing effects of many of the osmolytes. However, betaine and proline are predicted to be destabilizing, when experimentally we find these osmolytes act to stabilize the tetramer. Quantitatively, the model fails to accurately predict

dx.doi.org/10.1021/bi401049s | *Biochemistry* 2013, 52, 9367−9374

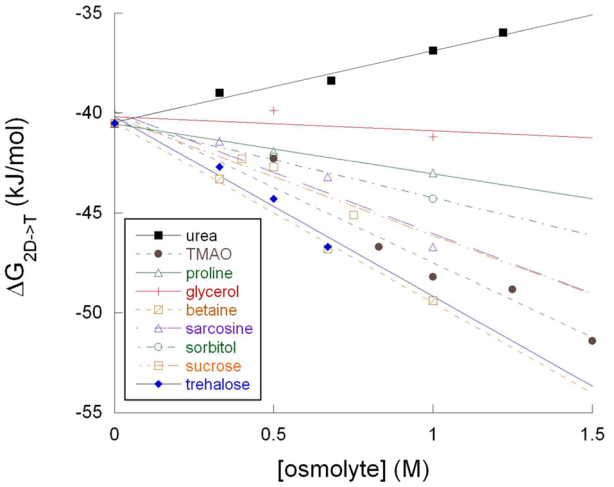

Figure 4. Association free energy as a function of osmolyte concentration. Slopes from linear fits give *m*-values shown in Table 1. The error in the association free energy was determined to be ±0.8 kJ/mol.

Table 1. Measured and Predicted *m*-Values for Nine Osmolytes (in kJ/(mol·M))

	measured m^a	experimental error^b	predicted m (TTM)^c	predicted m (Record)^d
urea	−3.58	0.29	−0.31	−2.06
TMAO	7.53	0.77	1.40	
sarcosine	6.11	1.2	1.63	
betaine	9.04	0.32	−1.90	3.47
proline	2.50	0.17	−1.24	3.12
glycerol	0.70	1.1	−0.29	
sorbitol	3.80	0.25	0.66	
sucrose	5.90	1.0	1.23	
trehalose	8.99	1.2	2.69	

[a]Determined from the slopes of the fitted lines in Figure 4. [b]Fitting error of the slopes using error bars of ±0.8 kJ/(mol·M) on the values of $\Delta G_{T\rightarrow 2D}$. [c]Calculated using the Tanford transfer model according to Methods. [d]Calculated using methods developed by Record and co-workers.[13,38,39]

the *m*-values in all cases but glycerol, in which case the experimentally determined *m*-value is within error of the prediction. For comparison, we also used surface area-based calculations for predicting the *m*-values for urea.[47] According to a recent analysis by Pace and co-workers, for 39 proteins lacking disulfide bonds, $m = 0.648 \times \Delta$SASA, with a correlation coefficient of 0.95.[48] This relationship predicts a urea *m*-value for ConA association of −2.6 kJ/(mol·M). This predicted *m*-value is much closer to the measured value than are the transfer model predictions, despite the simplicity and naiveté of this method (see Discussion). Record's procedure for predicting *m*-values did significantly better than the TTM, although the magnitudes, particularly for betaine, are still noticeably different from our experimental values. Our *m*-values are generally larger in magnitude than the theoretical predictions, but they are not aberrantly large (experimental *m*-values for monomeric protein folding typically range from 3 to 17 kJ/(mol·M)).[10]

DISCUSSION

The evolutionary process often identifies a mechanism to solve a particular biological problem and applies this solution broadly in a variety of organisms. Natural selection has afforded organisms a broad repertoire of versatile osmolytes from which to draw upon to meet species-level demands.[2] The success of this powerful regulatory strategy is possible by virtue of the system's reliance on simple fundamental physical commonalities among plethoric cellular microenvironments and their external conditions. These commonalities suggest that processes that rely on similar physical forces and phenomena, such as protein folding and association, will be affected similarly by common solution variables like the presence of osmolytes.

Previous studies of protein association and osmolytes have shown mixed results. Pielak and co-workers used saccharides as crowding agents and studied their effect on the dimerization of α-chymotrypsin.[49] They found a significant stabilization of the dimeric form (relative to monomer) by glucose, sucrose, and raffinose. They determined *m*-values ranging from 12 kJ/(mol·M) to 29 kJ/(mol·M) for these sugars. They also calculated an *m*-value for sucrose using the transfer model; however, the calculated effect of sucrose on the association constant was much lower in magnitude than what they observed experimentally. The same group also studied the complex of cytochrome *c* with cytochrome *c* oxidase and found only very small effects on stability of the complex by sugars (all *m*-values were within error of zero).[50] In this case the transfer model predicted the lack of effects with reasonable accuracy; however, the authors concluded that, in general, predictions of osmolyte action on protein−protein interfaces would need to consider factors not accounted for by the transfer model (see below). Chebotareva et al. examined the self-association of phosphorylase kinase and the association of phosphorylase kinase with phosphorylase b.[16] TMAO and betaine were found to strongly favor self-association; proline disfavored association, and all the osmolytes inhibited complex formation by the kinase and phosphorylase b. The limited amount of data on hand suggests that osmolytes that tend to stabilize the folding of protein subunits also stabilize protein−protein interfaces, and osmolytes that destabilize folded subunits (i.e., urea) destabilize interfaces, although exceptions exist and more are surely to be found. Naturally, further work on other oligomeric proteins and protein complexes is needed to determine if the stabilization of protein−protein interfaces observed here and in other studies is a general phenomenon.

A surprising simplicity becomes apparent upon considering the thermodynamic effect of osmolytes and denaturants on protein conformational changes. As first noted by Pace,[33] the effect of common denaturants such as urea or guanidine hydrochloride is empirically observed to be a linear function of denaturant concentration. Similar observations have been made for TMAO and its effect on folding disordered proteins as well as increasing the stability of folded proteins.[8,9] For denaturants, a strong correlation was noted between *m*-values and the change in accessible surface area (ΔSASA) upon protein unfolding.[47] As pointed out by Bolen and Rose,[51] this correlation is a result of indirect causation. According to experimentally measured transfer free energies, the main contributor to these *m*-values appears to be the polypeptide backbone (just as it is for stabilizing osmolytes). The ΔSASA for the backbone is correlated with the total ΔSASA, hence the correlation between *m*-values and total ΔSASA. Despite this caveat, the total ΔSASA of ConA association predicts the urea *m*-value better than does the transfer model, and urea *m*-values seem to be of use as general measures of ΔSASA in a wide variety of contexts.

dx.doi.org/10.1021/bi401049s | *Biochemistry* 2013, 52, 9367−9374

The Tanford transfer model, a long-standing method for understanding the effects of small molecules on protein folding, has been successfully used by Bolen and co-workers to predict *m*-values for a wide variety of osmolytes for the folding of several different monomeric proteins.[10] Why does the model fail for our system? One possibility is some hidden uniqueness regarding ConA. However, more likely explanations may be found by comparing the protein surface buried in the folding of monomeric proteins to that buried in the formation of noncovalent complexes. In protein folding, the surface area change is dominated by the burial not only of nonpolar side chains in the hydrophobic core but also of peptide groups by the formation of secondary structure and by the packing of elements of secondary structure together. Superficially, subunit interfaces resemble the interiors of folded monomeric proteins, in that they contain closely packed nonpolar side chains, hydrogen-bonded polar side chains, and other polar interactions like salt bridges and the like. However, protein−protein interfaces differ from subunit interiors in several respects,[52,53] including (i) their hydrophobicities are less than those of permanent interfaces, lying somewhere between those of interiors and exteriors, (ii) ∼77% of intersubunit hydrogen bonds are between side chains, while ∼68% of the hydrogen bonds within subunits are between backbone atoms (this difference is because of the discontinuation of secondary structural elements, with the occasional exception of β sheets, across subunit boundaries), (iii) many protein−protein interfaces contain salt bridges, contributing to the specificity and stability of subunit associations, whereas buried salt bridges in proteins are rare,[54] and (iv) buried, immobilized water molecules (typically hydrogen bonded to protein groups as part of an interaction network) are often integral parts of the interface.[55] Thus, it becomes apparent that protein−protein interfaces are quite different than the protein surfaces that are buried in monomeric interiors. The association of two protein subunits typically buries a surface area of 1000−2000 Å^2 (and no less than 600 Å^2) that would otherwise be exposed to solvent.[52,53] These values are much less than the typical amount of area that is buried upon folding of a monomeric subunit,[47,56] surely making molecular details more important.

Since interactions between polar side chains are particularly crucial in protein−protein interfaces, the TTM is vulnerable to problems associated with group additivity, which is a key assumption of the TTM. Additivity is present reliably for nonpolar groups.[57,58,57,58,58] There is a long-standing controversy regarding group additivity as applied to peptide groups;[59] however, treatments of peptide group models have been developed to give additive transfer free energies.[60] For the polar (and especially charged) side chains, we have doubts as to the applicability of additive group free energies.[61] If group additivity is failing for polar side chains, then it is easy to understand the failure of the model to predict *m*-values for ConA. In the dimer−dimer interface only 13% of the surface area buried is due to the backbone; most of the ΔSASA arises from side chain burial. A majority of the buried side chains are polar amino acids, and 36% of the total buried surface is from polar atoms on the side chains, compared to 10−15% for monomeric protein folding. Thus, a significant amount of the association free energy for ConA (and other protein−protein interfaces) is related to the burial of polar side chains; in this circumstance, the additivity assumption may be failing. In contrast, the TTM may work better for protein folding since those predictions are less reliant on accurate estimates of polar side chain transfer free energy. Most of the protein surface buried when a typical monomeric protein folds is due to nonpolar side chains and peptide groups, for which the assumption of additivity is more likely to hold. Record's model also assumes additivity, although the assumption can be rechecked against the model compound set used for a particular osmolyte. The interactions of the three osmolytes with the model compounds seem well-described by the sum of interaction energies with individual functional groups.[39]

Immobilized water molecules that are integral parts of the interfacial network of interactions in protein−protein interfaces may cause theoretical models particular difficulties. On average, 11 water molecules per 1000 Å^2 of buried surface are present in oligomeric interfaces, and 10 water molecules are present in that amount of area for interfaces in protein complexes.[53,55] These water molecules often act as "bridges," being hydrogen bonded to groups on both subunits. ConA is no exception, and a number of water molecules that appear to mediate the interactions between dimers (Figure 1B,C) are visible in the crystal structure. Since the presence of osmolytes leads to a variety of changes in protein hydration,[3,6,13,62] the thermodynamics of bringing these water molecules from the bulk solvent into the interface will undoubtedly be complex and will not be reflected by simple transfer free energies (or interaction parameters) of the groups involved.

Schellman, Pielak, and others have previously noted the importance of considering excluded volume when considering the mechanism of osmolyte action on protein association.[11,15,63] While the transfer model inherently contains information about the effect of excluded volume on protein groups, it does not account for exclusion caused by each protein on the other. While these steric effects can be estimated, there are several difficulties, including the need to treat the interacting species as being composed of hard, impenetrable spheres.[15]

There are several other explanations for the lack of theoretical success that may be specific for ConA. Although formation of the ConA tetramer from dimers appears to involve prefolded subunits, small conformational changes may be present in solution that are not detectable by crystallographic or spectroscopic methods or that result in an alteration of the saccharide binding affinity. Changes in SASA caused by these rearrangements would not be included in the theoretical models, and incomplete knowledge of the size and/or shape of the interaction surface would hinder the application of any detailed model. However, as noted above, the existing evidence seems to rule out major subunit conformational changes upon tetramer formation for ConA. Additionally, there is the possibility of specific binding of osmolytes to ConA. Stronger binding to either dimer or tetramer would naturally shift the association equilibrium. Now, the linearity of the free energy versus [osmolyte] plots (Figure 4) appears to rule out such binding, but it is difficult to totally eliminate specific binding as a contributor. Lastly, we need to consider the possibility that osmolytes perturb the pK_a of the histidine responsible for the pH dependence of the quaternary structure. Record's results suggest that osmolytes are preferentially excluded by some functional groups but included by others, and osmolytes may accumulate near the critical histidine side chain. We can only eliminate this last possibility by conclusively identifying and measuring the pK_a of the histidine in question as a function of osmolyte concentration.

A successful theory of osmotic action on protein association and binding will by necessity have to reckon with the sort of molecular details discussed above; unfortunately, in doing so the main advantage of the current theoretical models—relative simplicity—might be lost. To facilitate the development of such a model, further work in our lab will focus on the influence of osmolytes on the enthalpy, entropy, and heat capacity changes of ConA association, and we hope to undertake similar studies of additional protein−protein interfaces and protein interfaces with other types of molecules.

CONCLUSIONS

Osmolytes demonstrate similar effects on ConA association as they do on monomeric protein folding, although further work is needed to see if our observations are generally applicable to other protein−protein interfaces. The TTM fails to accurately predict *m*-values describing the effect of osmolytes on ConA self-association; the atomic-level details of protein−protein interfaces apparently cause difficulties for the model. Record's model does better, but further theoretical work is necessary to enhance our understanding of how this fascinating class of molecules influences the wide variety of protein interactions that are so essential for biological function.

ASSOCIATED CONTENT

Supporting Information

A table of changes in accessible surface area upon ConA association is available free of charge via the Internet at http://pubs.acs.org.

AUTHOR INFORMATION

Corresponding Author

*E-mail: jemyers@davidson.edu. Tel.: (704) 894-2304.

Funding

The authors wish to acknowledge Davidson College for funding of this project through its Center for Interdisciplinary Studies, the Chemistry Department, and Faculty Study and Research Grants.

Notes

The authors declare no competing financial interest.

ACKNOWLEDGMENTS

We wish to thank Eric Nicholson and Christopher Henkels for comments and advice, and two anonymous reviewers for their helpful suggestions.

ABBREVIATIONS

SASA, solvent-accessible surface area; CD, circular dichroism; ConA, concanavalin A; TTM, Tanford transfer model; TMAO, trimethyamine *N*-oxide

REFERENCES

(1) Yancey, P. H., Clark, M. E., Hand, S. C., Bowlus, R. D., and Somero, G. N. (1982) Living with water stress: evolution of osmolyte systems. *Science 217*, 1214−1222.

(2) Hochachka, P. W., Somero, G. N. *Biochemical Adaptation: Mechanism and Process in Physiological Evolution*; Oxford University Press: New York, 2002.

(3) Arakawa, T., and Timasheff, S. N. (1985) The stabilization of proteins by osmolytes. *Biophys. J. 47*, 411−414.

(4) Wang, A., and Bolen, D. W. (1997) A naturally occurring protective system in urea-rich cells: mechanism of osmolyte protection of proteins against urea denaturation. *Biochemistry 36*, 9101−9108.

(5) Saunders, A. J., Davis-Searles, P. R., Allen, D. L., Pielak, G. J., and Erie, D. A. (2000) Osmolyte-induced changes in protein conformational equilibria. *Biopolymers 53*, 293−307.

(6) Courtenay, E. S., Capp, M. W., Anderson, C. F., and Record, M. T., Jr. (2000) Vapor pressure osmometry studies of osmolyte−protein interactions: implications for the action of osmoprotectants in vivo and for the interpretation of "osmotic stress" experiments in vitro. *Biochemistry 39*, 4455−4471.

(7) Bolen, D. W., and Baskakov, I. V. (2001) The osmophobic effect: natural selection of a thermodynamic force in protein folding. *J. Mol. Biol. 310*, 955−963.

(8) Henkels, C. H., Kurz, J. C., Fierke, C. A., and Oas, T. G. (2001) Linked folding and anion binding of the *Bacillus subtilis* ribonuclease P protein. *Biochemistry 40*, 2777−2789.

(9) Mello, C. C., and Barrick, D. (2003) Measuring the stability of partly folded proteins using TMAO. *Protein Sci. 12*, 1522−1529.

(10) Auton, M., Rosgen, J., Sinev, M., Holthauzen, L. M., and Bolen, D. W. (2011) Osmolyte effects on protein stability and solubility: A balancing act between backbone and side-chains. *Biophys. Chem. 159*, 90−99.

(11) Schellman, J. A. (2003) Protein stability in mixed solvents: a balance of contact interaction and excluded volume. *Biophys. J. 85*, 108−125.

(12) Street, T. O., Bolen, D. W., and Rose, G. D. (2006) A molecular mechanism for osmolyte-induced protein stability. *Proc. Natl. Acad. Sci. U.S.A. 103*, 13997−14002.

(13) Capp, M. W., Pegram, L. M., Saecker, R. M., Kratz, M., Riccardi, D., Wendorff, T., Cannon, J. G., and Record, M. T., Jr. (2009) Interactions of the osmolyte glycine betaine with molecular surfaces in water: thermodynamics, structural interpretation, and prediction of *m*-values. *Biochemistry 48*, 10372−10379.

(14) Holthauzen, L. M., Rosgen, J., and Bolen, D. W. (2010) Hydrogen bonding progressively strengthens upon transfer of the protein urea-denatured state to water and protecting osmolytes. *Biochemistry 49*, 1310−1318.

(15) Patel, C. N., Noble, S. M., Weatherly, G. T., Tripathy, A., Winzor, D. J., and Pielak, G. J. (2002) Effects of molecular crowding by saccharides on α-chymotrypsin dimerization. *Protein Sci. 11*, 997−1003.

(16) Chebotareva, N. A., Andreeva, I. E., Makeeva, V. F., Livanova, N. B., and Kurganov, B. I. (2004) Effect of molecular crowding on self-association of phosphorylase kinase and its interaction with phosphorylase b and glycogen. *J. Mol. Recognit. 17*, 426−432.

(17) Olson, M. O. J., and Liener, I. E. (1967) Some physical and chemical properties of concanavalin a phytohemagglutinin of jack bean. *Biochemistry 6*, 105−111.

(18) Agrawal, B. B., and Goldstein, I. J. (1968) Protein-carbohydrate interaction. VII. Physical and chemical studies on concanavalin A, the hemagglutinin of the jack bean. *Arch. Biochem. Biophys. 124*, 218−229.

(19) Weis, W. I., and Drickamer, K. (1996) Structural basis of lectin−carbohydrate recognition. *Annu. Rev. Biochem. 65*, 441−473.

(20) Hardman, K. D., and Ainswort, C. F. (1972) Structure of concanavalin A at 2.4 angstrom resolution. *Biochemistry 11*, 4910−4919.

(21) Reeke, G. N., Jr, Becker, J. W., and Edelman, G. M. (1975) The covalent and three-dimensional structure of concanavalin A. IV. Atomic coordinates, hydrogen bonding, and quaternary structure. *J. Biol. Chem. 250*, 1525−1547.

(22) Becker, J. W., Reeke, G. N., Jr, Wang, J. L., Cunningham, B. A., and Edelman, G. M. (1975) The covalent and three-dimensional structure of concanavalin A. III. Structure of the monomer and its interactions with metals and saccharides. *J. Biol. Chem. 250*, 1513−1524.

(23) Parkin, S., Rupp, B., and Hope, H. (1996) Atomic resolution structure of concanavalin A at 120 K. *Acta Crystallogr., Sect. D: Biol. Crystallogr. 52*, 1161−1168.

(24) Chatterjee, A., and Mandal, D. K. (2003) Denaturant-induced equilibrium unfolding of concanavalin A is expressed by a three-state

mechanism and provides an estimate of its protein stability. *Biochim. Biophys. Acta 1648*, 174−183.
(25) Mitra, N., Srinivas, V., Ramya, T., Ahmad, N., Reddy, G., and Surolia, A. (2002) Conformational stability of legume lectins reflect their different modes of quaternary association: solvent denaturation studies on concanavalin A and winged bean acidic agglutinin. *Biochemistry 41*, 9256−9263.
(26) Senear, D. F., and Teller, D. C. (1981) Effects of saccharide and salt binding on dimer−tetramer equilibrium of concanavalin A. *Biochemistry 20*, 3083−3091.
(27) Mandal, P., and Mandal, D. K. (2011) Localization and environment of tryptophans in different structural states of concanavalin A. *J. Fluoresc. 21*, 2123−2132.
(28) Senear, D. F., and Teller, D. C. (1981) Thermodynamics of concanavalin A dimer−tetramer self-association: sedimentation equilibrium studies. *Biochemistry 20*, 3076−3083.
(29) Zand, R., Agrawal, B. B., and Goldstein, I. J. (1971) pH-dependent conformational changes of concanavalin A. *Proc. Natl. Acad. Sci. U.S.A. 68*, 2173−2176.
(30) Huet, M., and Claverie, J. M. (1978) Sedimentation studies of reversible dimer−tetramer transition kinetics of concanavalin A. *Biochemistry 17*, 236−241.
(31) Herskovits, T. T., Jacobs, R., and Nag, K. (1983) The effects of salts and ureas on the subunit dissociation of concanavalin A. *Biochim. Biophys. Acta 742*, 142−154.
(32) Tanford, C. (1970) Protein denaturation: Part C. Theoretical models for the mechanism of denaturation. *Adv. Prot. Chem. 24*, 1−95.
(33) Greene, R. F., Jr, and Pace, C. N. (1974) Urea and guanidine hydrochloride denaturation of ribonuclease, lysozyme, α-chymotrypsin, and β-lactoglobulin. *J. Biol. Chem. 249*, 5388−5393.
(34) Pace, C. N., and Shaw, K. L. (2000) Linear extrapolation method of analyzing solvent denaturation curves. *Proteins 4* (Suppl), 1−7.
(35) Santoro, M. M., and Bolen, D. W. (1992) A test of the linear extrapolation of unfolding free energy changes over an extended denaturant concentration range. *Biochemistry 31*, 4901−4907.
(36) Nicholson, E. M., and Scholtz, J. M. (1996) Conformational stability of the *Escherichia coli* HPr protein: test of the linear extrapolation method and a thermodynamic characterization of cold denaturation. *Biochemistry 35*, 11369−11378.
(37) Mello, C. C., and Barrick, D. (2003) Measuring the stability of partly folded proteins using TMAO. *Protein Sci. 12*, 1522−1529.
(38) Guinn, E. J., Pegram, L. M., Capp, M. W., Pollock, M. N., and Record, M. T., Jr. (2011) Quantifying why urea is a protein denaturant, whereas glycine betaine is a protein stabilizer. *Proc. Natl. Acad. Sci. U.S.A. 108*, 16932−16937.
(39) Diehl, R. C., Guinn, E. J., Capp, M. W., Tsodikov, O. V., and Record, M. T., Jr. (2013) Quantifying additive interactions of the osmolyte proline with individual functional groups of proteins: comparisons with urea and glycine betaine, interpretation of *m*-values. *Biochemistry 52*, 5997−6010.
(40) Cunningham, B. A., Wang, J. L., Pflumm, M. N., and Edelman, G. M. (1972) Isolation and proteolytic cleavage of the intact subunit of concanavalin A. *Biochemistry 11*, 3233−3239.
(41) Shaw, K. L., Scholtz, J. M., Pace, C. N., and Grimsley, G. R. (2009) Determining the conformational stability of a protein using urea denaturation curves. *Methods Mol. Biol. 490*, 41−55.
(42) Celinski, S. A., and Scholtz, J. M. (2002) Osmolyte effects on helix formation in peptides and the stability of coiled-coils. *Protein Sci. 11*, 2048−2051.
(43) Wyman, J. (1964) Linked functions and reciprocal effects in hemoglobin: a second look. *Adv. Protein Chem. 19*, 223−286.
(44) Auton, M., and Bolen, D. W. (2005) Predicting the energetics of osmolyte-induced protein folding/unfolding. *Proc. Natl. Acad. Sci. U.S.A. 102*, 15065−15068.
(45) Auton, M., Holthauzen, L. M., and Bolen, D. W. (2007) Anatomy of energetic changes accompanying urea-induced protein denaturation. *Proc. Natl. Acad. Sci. U.S.A. 104*, 15317−15322.
(46) Auton, M., and Bolen, D. W. (2007) Application of the transfer model to understand how naturally occurring osmolytes affect protein stability. *Methods Enzymol. 428*, 397−418.
(47) Myers, J. K., Pace, C. N., and Scholtz, J. M. (1995) Denaturant *m*-values and heat capacity changes: relation to changes in accessible surface areas of protein unfolding. *Protein Sci. 4*, 2138−2148.
(48) Pace, C. N., Huyghues-Despointes, B. M., Fu, H., Takano, K., Scholtz, J. M., and Grimsley, G. R. (2010) Urea denatured state ensembles contain extensive secondary structure that is increased in hydrophobic proteins . *Protein Sci. 19*, 929−943.
(49) Winzor, D. J., Patel, C. N., and Pielak, G. J. (2007) Reconsideration of sedimentation equilibrium distributions reflecting the effects of small inert cosolutes on the dimerization of α-chymotrypsin. *Biophys. Chem. 130*, 89−92.
(50) Morar, A. S., Wang, X., and Pielak, G. J. (2001) Effects of crowding by mono-, di-, and tetrasaccharides on cytochrome *c*-cytochrome *c* peroxidase binding: comparing experiment to theory. *Biochemistry 40*, 281−285.
(51) Bolen, D. W., and Rose, G. D. (2008) Structure and energetics of the hydrogen-bonded backbone in protein folding. *Annu. Rev. Biochem. 77*, 339−362.
(52) Janin, J., Miller, S., and Chothia, C. (1988) Surface, subunit interfaces, and interior of oligomeric proteins. *J. Mol. Biol. 204*, 155−164.
(53) Janin, J., Bahadur, R. P., and Chakrabarti, P. (2008) Protein−protein interaction and quaternary structure. *Q. Rev. Biophys. 41*, 133−180.
(54) Miller, S., Janin, J., Lesk, A. M., and Chothia, C. (1987) Interior and surface of monomeric proteins. *J. Mol. Biol. 196*, 641−656.
(55) Rodier, F., Bahadur, R. P., Chakrabarti, P., and Janin, J. (2005) Hydration of protein−protein interfaces. *Proteins 60*, 36−45.
(56) Miller, S., Janin, J., Lesk, A. M., and Chothia, C. (1987) Interior and surface of monomeric proteins. *J. Mol. Biol. 196*, 641−656.
(57) Tanford, C. *The Hydrophobic Effect: Formation of Micelles and Biological Membranes*; John Wiley & Sons: New York, 1980.
(58) Graziano, G., and Barone, G. (1996) Group additivity analysis of the heat capacity changes associated with the dissolution into water of different organic compounds. *J. Am. Chem. Soc. 118*, 1831−1835.
(59) Avbelj, F., and Baldwin, R. L. (2006) Limited validity of group additivity for the folding energetics of the peptide group. *Proteins 63*, 283−289.
(60) Auton, M., and Bolen, D. W. (2004) Additive transfer free energies of the peptide backbone unit that are independent of the model compound and the choice of concentration scale. *Biochemistry 43*, 1329−1342.
(61) Chang, J., Lenhoff, A. M., and Sandler, S. I. (2007) Solvation free energy of amino acids and side-chain analogues. *J. Phys. Chem. B 111*, 2098−2106.
(62) Auton, M., Bolen, D. W., and Rosgen, J. (2008) Structural thermodynamics of protein preferential solvation: osmolyte solvation of proteins, aminoacids, and peptides. *Proteins 73*, 802−813.
(63) Sarkar, M., Lee, C., and Pielak, G. J. (2013) Soft interactions and crowding. *Biophys. Rev. 5*, 187−194.
(64) Pettersen, E. F., Goddard, T. D., Huang, C. C., Couch, G. S., Greenblatt, D. M., Meng, E. C., and Ferrin, T. E. (2004) UCSF Chimera—a visualization system for exploratory research and analysis. *J. Comput. Chem. 25*, 1605−1612.